



OPEN

Deep learning-based prediction of early cerebrovascular events after transcatheter aortic valve replacement

Taishi Okuno^{1,3}, Pavel Overtchouk^{1,2,3}✉, Masahiko Asami¹, Daijiro Tomii¹, Stefan Stortecky¹, Fabien Praz¹, Jonas Lanz¹, George C. M. Siontis¹, Christoph Gräni¹, Stephan Windecker¹ & Thomas Pilgrim¹

Cerebrovascular events (CVE) are among the most feared complications of transcatheter aortic valve replacement (TAVR). CVE appear difficult to predict due to their multifactorial origin incompletely explained by clinical predictors. We aimed to build a deep learning-based predictive tool for TAVR-related CVE. Integrated clinical and imaging characteristics from consecutive patients enrolled into a prospective TAVR registry were analysed. CVE comprised any strokes and transient ischemic attacks. Predictive variables were selected by recursive feature reduction to train an autoencoder predictive model. Area under the curve (AUC) represented the model's performance to predict 30-day CVE. Among 2279 patients included between 2007 and 2019, both clinical and imaging data were available in 1492 patients. Median age was 83 years and STS score was 4.6%. Acute (<24 h) and subacute (day 2–30) CVE occurred in 19 (1.3%) and 36 (2.4%) patients, respectively. The occurrence of CVE was associated with an increased risk of death (HR [95% CI] 2.62 [1.82–3.78]). The constructed predictive model uses less than 107 clinical and imaging variables and has an AUC of 0.79 (0.65–0.93). TAVR-related CVE can be predicted using a deep learning-based predictive algorithm. The model is implemented online for broad usage.

Deep learning is a subset of machine learning where artificial neural networks, algorithms inspired by the structure and function of the human brain, learn complex relationships from large amounts of data to make accurate predictions^{1,2}. In certain fields, artificial neural networks have been shown to exceed human abilities^{1,2}. The ability of deep learning to recognize patterns and learn valuable features from raw input data without requiring human intervention has a potential to help in acquiring, interpreting, and synthesizing growing medical data to improve clinical care³. Thus, deep learning is now increasingly investigated and utilized in the medical field, of which cardiovascular medicine is no exception^{4,5}. As a wide variety of data such as clinical data, laboratory data, imaging data, and procedural data needs to be integrated and considered for preprocedural planning, performing, and post-procedural care of transcatheter aortic valve replacement (TAVR), the field may particularly benefit from the implementation of deep learning^{6–8}.

Cerebrovascular events (CVE) are rare but yet the most feared complications in patients undergoing TAVR⁹. Despite continuous improvements in technique and devices, the risk of CVE remains fairly stable across randomized as well as observational studies^{10,11}. Hence, the challenge of CVE prevention is an unmet clinical need and will gain particular topicality with the extension of TAVR to lower risk and younger patients at hand. Histological analysis of debris captured by cerebral protection devices during TAVR has shown that not only thrombus, but also aortic valve and wall tissue, calcium and connective tissue embolize in the cerebrovascular circulation during the procedure, suggesting multiple and complex mechanisms of CVE in patients undergoing TAVR¹². Although several independent risk factors, such as atherosclerosis, atrial fibrillation, use of balloon dilatation, and device dislocation or embolization have been suggested^{9,13–18}, no predictive tool regrouping all possible contributing factors has been proposed so far. This might be because conventional statistical approaches such as

¹Department of Cardiology, Inselspital, Bern University Hospital, University of Bern, Bern, Switzerland. ²AlvissLabs Research, ALVISS.AI SAS, 29 rue Oudry, 75013 Paris, France. ³These authors contributed equally: Taishi Okuno and Pavel Overtchouk. ✉email: pavel@alviss.ai

logistic regression fail to integrate the multifactorial interactive relationship of numerous possible predictors of CVE which statistically remain “rare” events.

We therefore aimed to apply a deep learning method to develop a predictive model for CVE after TAVR.

Methods

Study population. Between August 2007 and February 2019, clinical, procedural and follow-up data of 2279 consecutive patients undergoing TAVR for aortic stenosis were prospectively enrolled into an institutional registry that forms part of the Swiss TAVR registry (NCT01368250)¹¹. For the purpose of the present study, we selected patients with adequate preprocedural multi-detector computed tomography (MDCT) data from the registry as we hypothesized that imaging data is important for CVE predicting modelling.

The indication for TAVR was decided based on the evaluation of the local Heart Team. The procedure was performed according to standardized protocols regarding the access site, type and size of the device, based on a comprehensive evaluation of clinical, biological and anatomical characteristics as per echocardiography and MDCT for each patient at baseline. Procedural anticoagulation was achieved with administration of intravenous heparin at an initial dose of 5000 IU or 70 IU/kg, aiming at an activated clotting time (ACT) of 250–300 seconds. The preferred antithrombotic treatment after TAVR comprised dual antiplatelet therapy (aspirin and clopidogrel) for 6 months followed by lifelong aspirin in patients without indication for oral anticoagulation, but ticagrelor or prasugrel were accepted in presence of concomitant indication such as recent percutaneous coronary revascularisation. In patients with atrial fibrillation or other indication for oral anticoagulation, the anti-thrombotic regimen comprised an anticoagulant agent alone or a combination with single or dual antiplatelet therapy as tailored according to patient comorbidities. The registry and the study protocol are approved by the Bern cantonal ethics committee and all participants provided written informed consent prior to inclusion. The study was conducted in compliance with the Declaration of Helsinki.

Computed tomography evaluation. Contrast-enhanced ECG-gated MDCT examinations were performed on either a Siemens Somatom Sensation Cardiac 64 scanner with a slice collimation of 1.5 mm or a Siemens Somatom Definition Flash Dual-Source scanner with a slice collimation of 0.6 mm, tube voltage of 100 or 120 kV, and tube current according to patient size (Siemens Medical Solutions, Inc., Forchheim, Germany) as previously described¹⁹. Acquired CT images were independently re-evaluated on a dedicated workstation (3mensio Structural Heart, 3mensio Medical Imaging BV, Bilthoven, The Netherlands). Basic measurements were made in accordance with a current expert consensus document²⁰. Calcium volume in the aortic valve complex and mitral valve complex were measured as previously described^{19,21}. Ascending aorta length is defined in the presented study as the distance at which the line drawn perpendicular to the aortic valve annulus plane hits the ascending aortic wall (Fig. 1).

Study objectives. The primary objective of this study was to build a predictive model for TAVR-related CVE. We also aimed to investigate the relative importance of clinical and CT imaging variables for CVE risk prediction, and to evaluate the impact of CVE on mortality.

The primary endpoint was the area under the receiver operating curve (AUC), the most widely used measure of global performance of predictive models.

Clinical endpoints/outcomes. All data were entered into a dedicated web-based database held at the Clinical Trials Unit of the University of Bern. A clinical event committee adjudicated all adverse events based on the Valve Academic Research Consortium (VARC) criteria²². Vital status and date of censoring or death were recorded in the registry.

All CVE, including any stroke and transient ischemic attack (TIA), were recorded. Whenever stroke or TIA was suspected, patients underwent examination by a board-certified neurologist and underwent diagnostic neuroimaging at his/her discretion. Stroke and transient ischaemic attack were defined in accordance with the definition of a central nervous system (CNS) type 1 and type 3a event, respectively (ARC)²³. Stroke events were further subdivided into disabling and non-disabling as per VARC-2²². We hypothesized that TAVR related CVE occurred within 30 days after the procedures and considered all acute and subacute CVE as the primary outcome for predictive modelling.

Deep learning predictive modelling. Machine learning modeling refers to the development of a mathematical representation of data by a training process. Given the highly unbalanced character of the predicted class (only 3.7% of patients presented a 30-day CVE versus 96.3% did not) we chose a rare-event autoencoder to be the prediction model²⁴.

The rare event autoencoder is made of 2 modules of neural networks: encoder and decoder. The former learns the underlying features representing the input data while the latter tries to recreate the original data from the features learned. The model is trained using the data of patients who did not present an event. When confronted with new data a reconstruction mean squared error (MSE) between the predicted data and the ground truth was used to estimate the risk of CVE. When the MSE is above a specified threshold we consider that the patient is at risk of CVE. Clinically it corresponds to an estimation of how a given patient differs from the population that usually does not develop a 30-day CVE regarding a range of clinical, biological and imaging characteristics. The threshold is chosen from the analysis of the precision-recall curve of the validation data (Supplementary Fig. 1).

Categorical variables were entered in the model after one-hot-encoding pre-processing. Variable importance was used for variable selection and estimated based on the impact of its neutralization (median value for

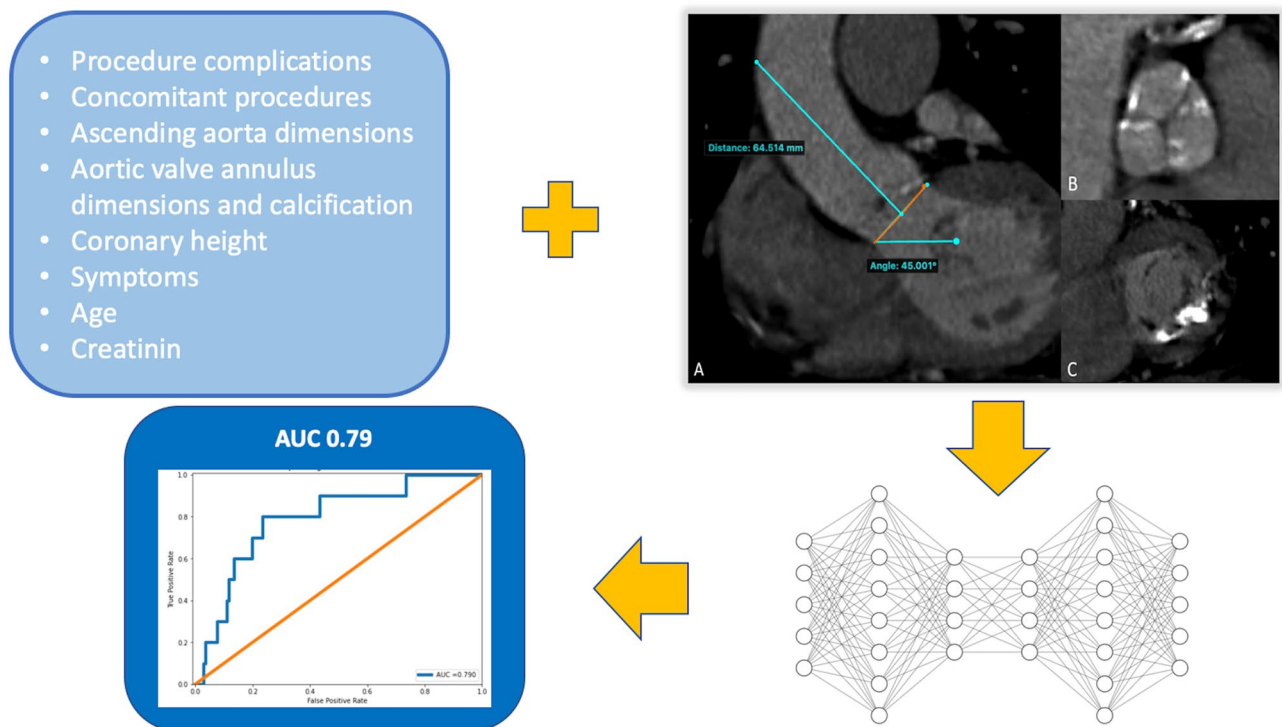


Figure 1. Graphic representation of the presented predictive model. CT imaging and other clinical data are entered in the autoencoder predictive model to yield an estimation of the risk of a cerebrovascular event (stroke or transient ischemic attack). (A) CT sagittal view of the ascending aorta and left ventricular outflow tract. In orange is presented the aortic annulus plane. In cyan are presented the ascending aorta length and the annulus angulation. (B) transverse view of aortic valve cusps with calcium in the setting of a degenerative aortic stenosis. (C) transverse view of a mitral valve with calcium. Ascending aorta length: distance at which the line drawn perpendicular to the aortic valve annulus hits the ascending aortic wall (important note: this is different from the usual measurement which corresponds to the distance between the brachio-cephalic trunc and the aortic annulus). Right coronary cusp height: perpendicular distance between the outflow of the right coronary and the aortic annulus. The autoencoder model is represented here by a simplified schema.

continuous variables and 0 for categorical variables) on model performance. The selected variables are displayed ranked by importance in Supplementary Table 2 and Fig. 2.

Statistical analysis. Continuous and categorical variables are presented as medians (interquartile range) and as counts (percentage). Those were assessed with Mann–Whitney U test for continuous variables, and Chi square or Fisher exact test as appropriate for categorical variables. Collinearity was assessed prior to model building by analysis of the correlation matrix. Missing values ranged from 3.2 to 17.5% (overall 7.6%) and were treated with multiple imputations by a Monte Carlo dropout autoencoder²⁵.

Model performance was evaluated on the test set calculating the AUC. The overall database was randomly split into a train dataset (2/3 of total) used for model training and an independent test dataset (1/3) used for performance evaluation. The validation set represented 20% of the training set. The model was trained using python 3.7.9 and keras 2.4.3 software on MacBook Pro 2.4 GHz 8-Core Intel Core i9.

Python 3.7.9 (Python Software Foundation), R 3.6.1 (R Core Team, R A language and environment for statistical computing, R Foundation for Statistical Computing (Vienna, Austria). URL <https://www.R-project.org/>) and SPSS 23 (IBM SPSS Statistics for Windows, Version 23.0 Armonk, NY: IBM Corp) software were used to perform the statistical and machine learning analysis. P value < 0.05 was considered significant unless otherwise specified.

Results

Out of a total of 2279 patients included in the Bern TAVR database, 1492 patients had complete clinical and MDCT data (65%) (Fig. 2). Baseline characteristics are summarized in Tables 1 and 2. The median age of the population was 83.2 years (interquartile range [IQR] 79.4–86) and 48% were female. Twelve percent of patients had a history of prior stroke or TIA, and one third of patients had a history of atrial fibrillation. After a median duration of follow-up of 3 (1–4.3) years, 105 patients had experienced at least one CVE (7.8%) during the follow-up period. CVE occurred within the first 24 h in 19 patients (acute CVE), and between day 1 and day 30 in 36 patients (subacute CVE), accounting for a total of 55 events (3.7%) between the procedure and 30 days. Event-free survival rates for CVE were 96.3% (95% CI 95.3–97.3) at 30 days, 94.6% (95% CI 93.3–95.7) at 1 year, and 92.9% (91.5–94.3) at 2 years. Acute CVE were disabling strokes in 79% of cases (Table 3). The risk of CVE peaked within the first 24 h and levelled off within the first month, after which the risk of CVE remained stable

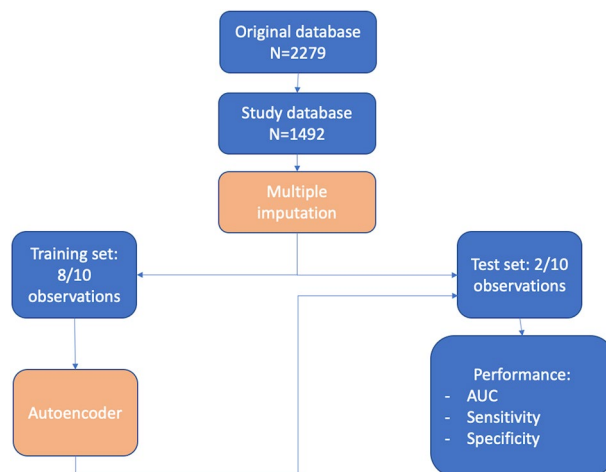


Figure 2. Study flow chart.

over time (Fig. 3). All-cause mortality during the observation period amounted to 32.6% (95% CI 30–35.2%), and the occurrence of CVE within 30 days was associated with an increased risk of death (univariate HR [95% CI] 2.62 [1.82–3.78], $P < 0.001$) (Fig. 4).

TAVR-related CVE predictive model. An extensive set (> 100 variables) of clinical, biological, imaging, and procedural characteristics as well as complications were considered for the deep learning predictive modelling (Tables 1, 2). Recursive feature elimination by variable importance suggested a drop in predictive performance when less than the 63 variables were included in the model (Supplementary Fig. 2). The trained model included 2 hidden layers in the encoder and decoder and used MDCT data (variables represented aortic calcium volume, aortic annulus and left ventricular outflow tract dimensions, ascending aorta dimensions and angulation), along with other clinical data (Fig. 1, Supplementary Fig. 2, Supplementary Tables 1, 2). The constructed predictive model had an AUC of 0.79 (0.65–0.93) (Fig. 5).

Discussion

Herein we propose a novel predictive model for TAVR-related CVE. The proposed model implements the deep neural network-type of algorithm and yields a satisfactory predictive performance with an AUC of 0.79 (0.65–0.93). Our study also suggests that imaging data could be as important as clinical characteristics for the construction of predictive models for cardiovascular procedures, although both types of variables are used in synergy by the constructed model developed for CVE.

CVE remains one of the most feared adverse events complicating TAVR. Despite fifteen years of improvement of the technique and refinement of TAVR devices, the occurrence of CVE during the peri-operative period remains notable^{10,11}. Preventive strategies for TAVR-related CVE are yet to provide evidence for their effectiveness. Cerebral protection devices have so far not been proven to reduce the risk of clinical CVE and none of the investigated antithrombotic strategies has shown protective effects in clinical investigations^{26–29}. The need for further investigation has been underscored by the Academic Research Consortium Initiative consensus proposing a standardized neurological endpoint evaluation for clinical research (NeuroARC)²³.

Previous studies have identified various risk factors for CVE in patients undergoing TAVR, which included clinical data such as atrial fibrillation and history of CVE, imaging data such as calcification of the aortic valve complex and reduced native and prosthetic aortic valve area, and procedural data such as balloon dilatation and device dislocation or embolization^{9,13–18}, however, a prediction model for CVE integrating all these factors have not been developed to date. Our data suggest an intricate relationship between clinical characteristics, anatomical features, peri-interventional antithrombotic management, and procedural complications to yield an overall risk estimation for CVE^{30,31}. Albeit severe, CVE after TAVR is an infrequent event which renders the classical predictive approach based on univariate then multivariable regression techniques difficult to implement. The multifactorial nature of TAVR-related CVE makes this approach further difficult. As suggested in our study, a justified deep learning approach has the potential to overcome such difficulties. Although, imaging parameters have not been identified as associated with CVE on conventional univariate analysis (Table 2), the autoencoder model exploited them to yield a satisfactory predictive performance. More interestingly, we observed a synergic exploitation of imaging data along clinical characteristics which suggests that predictive modelling could benefit from the inclusion of diverse types of data for their complementarity. This is, to the best of our knowledge, the first study proposing a predictive tool for TAVR-related CVE. The constructed model has been implemented by means of an open source online calculator (<https://www.welcome.alviss.ai/#/cvecalculator>). This online calculator may help improve risk stratification of patients undergoing TAVR and tailor subsequent follow-up and management strategies by recognizing high risk of CVE.

Precision medicine aims at adapting decision to a patient given his/her characteristics intended for a deep phenotyping. Machine learning models allow a holistic approach by analysing complex interactions between an

	Total (n = 1492)	No CVE (n = 1437)	CVE (n = 55)	P value
Female, n (%)	711 (47.7)	685 (47.7)	26 (47.3)	0.99
Age, years	83.2 (79.4–86)	83.1 (79.4–86.1)	83.4 (79.3–87.4)	0.27
Height, cm	165 (159–172)	165 (159–172)	165 (160–17)	0.67
Weight, kg	71 (62–82)	71 (62–82)	67 (59–84.5)	0.28
STS-PROM (%)	4.6 (3.2–7.0)	4.6 (3.1–7.0)	4.6 (3.1–7.0)	0.45
Concomitant diseases/history				
Hypertension, n (%)	1268 (85.0)	1219 (84.8)	49 (89.1)	0.49
Dyslipidemia, n (%)	975 (65.3)	941 (65.5)	34 (61.8)	0.67
Diabetes mellitus, n (%)	370 (24.8)	363 (25.3)	7 (12.7)	0.051
Dialysis, n (%)	30 (2.0)	29 (2.0)	1 (1.8)	0.99
Chronic obstructive pulmonary disease, n (%)	195 (13.1)	187 (13)	8 (14.5)	0.89
Coronary artery disease, n (%)	945 (63.3)	910 (63.3)	35 (63.6)	0.99
History of cardiac surgery, n (%)	224 (15.0)	216 (15.0)	8 (14.5)	0.99
Angina pectoris CCS 3 or 4, n (%)	118 (7.9)	113 (7.8)	5 (9.1)	0.54
Prior syncope, n (%)	183 (12.3)	175 (12.2)	8 (14.5)	0.75
Prior stroke/TIA, n (%)	174 (11.7)	162 (11.3)	12 (21.8)	0.029
Prior carotid artery disease, n (%)	168 (11.3)	155 (10.8)	13 (23.6)	0.006
Peripheral artery disease, n (%)	220 (14.7)	209 (14.5)	11 (20)	0.35
Atrial fibrillation, n (%)	492 (33)	471 (32.8)	21 (38.2)	0.49
Previous pacemaker implantation, n (%)	139 (9.3)	134 (9.3)	5 (9.1)	0.99
Medication at baseline				
Aspirin, n (%)	929 (62.3)	894 (62.2)	35 (63.6)	0.94
Clopidogrel, n (%)	273 (18.3)	265 (18.4)	8 (14.5)	0.57
Prasugrel, n (%)	7 (0.5)	7 (0.5)	0	0.99
Ticagrelor, n (%)	30 (2)	29 (2.0)	1 (1.8)	0.99
Oral anticoagulation, n (%)	431 (28.9)	410 (28.5)	21 (38.2)	0.16
Statin, n (%)	784 (52.5)	758 (52.7)	26 (47.3)	0.50
Laboratory values				
Creatinine, $\mu\text{mol/L}$	90 (74–112)	90 (74–111)	95 (79–120.5)	0.128
Haemoglobin, g/L	122.50 (111–133)	123 (111–133)	118 (110–130)	0.21
Thrombocytes, $10^3/\text{mm}^3$	212 (172–259)	212 (172–259)	203 (173.5–252.50)	0.72
Echocardiographic characteristics				
Mean aortic valve gradient, mmHg	40 (29, 5)	40 (29, 5)	41 (33.5, 54)	0.27
Left ventricle ejection fraction, %	60 (45, 65)	60 (45, 65)	60 (46.50, 65)	0.36
Mitral regurgitation grade III or IV, n (%)	284 (19.2)	270 (18.7)	15 (27.3)	0.46
Procedural characteristics				
Main Access				
Transfemoral, n (%)	1294 (86.7)	1247 (86.8)	47 (85.5)	0.90
Transapical, n (%)	180 (12.1)	173 (12.0)	7 (12.7)	
Other, n (%)	18 (1.2)	17 (1.2)	1 (1.8)	
Concomitant procedure				
PCI, n (%)	175 (11.7)	168 (11.7)	7 (12.7)	0.98
non-PCI interventions, n (%)	68 (4.6)	63 (4.4)	5 (9.1)	0.18
Type of valve				
Balloon-expandable, n (%)	683 (45.8)	657 (45.7)	26 (47.3)	0.96
Self-expanding, n (%)	688 (46.1)	663 (46.1)	25 (45.5)	
Mechanically expandable, n (%)	121 (8.1)	117 (8.1)	4 (7.3)	

Table 1. Patient clinical characteristics by occurrence of cerebrovascular event within 30 days after TAVR. Balloon-expandable valves: SAPIEN, SAPIEN XT, or SAPIEN 3 (Edwards Lifesciences, Irvine, CA, USA). Self-expanding valves: CoreValve, Evolut R/PRO (Medtronic, Minneapolis, MN, USA), Portico (Abbott, Chicago, IL, USA), or Symetis ACURATE.ACURATE neo (Boston Scientific, Marlborough, MA, USA). Mechanically-expanding valves: Lotus (Boston Scientific, Marlborough, MA, USA). CCS Canadian Cardiovascular Society grading, CVE cerebrovascular event, PCI percutaneous coronary intervention, STS-PROM Society of Thoracic Surgeons Predicted Risk of Mortality, TIA Transient ischemic attack.

	Total (n = 1492)	No CVE (n = 1437)	CVE (n = 55)	P value
Bicuspid valve on MDCT, n (%)	398 (26.7)	386 (26.8)	12 (21.8)	0.41
Maximal annular diameter, mm	26.8 (24.3–28.8)	26.8 (24.2–28.8)	27.3 (25.9–29.1)	0.20
Minimal annular diameter, mm	21.3 (19.7–23.6)	21.4 (19.7–23.6)	21 (19.2–22.9)	0.28
Mean annular diameter, mm	23.7 (21.9–25.4)	23.7 (21.9–25.4)	23.8 (22.6–25.3)	0.30
Annulus area, cm ²	431.4 (352.5–496.6)	431.4 (351.6–496.2)	441.2 (384–503.8)	0.28
Annulus perimeter, mm	77.8 (73.3–85.2)	77.8 (73.3–85.2)	78.1 (74.2–84.6)	0.95
Annulus eccentricity	0.78 (0.73–0.84)	0.78 (0.73–0.84)	0.76 (0.71–0.81)	0.052
Left coronary artery height, mm	15.3 (12.9–18.8)	15.3 (12.9–18.5)	15.1 (12.9–17.9)	0.86
Right coronary artery height, mm	16.9 (14.7–19.3)	16.9 (14.6–19.3)	17 (15.6–18.9)	0.75
Ascending aorta diameter, mm	32.3 (29.4–34.9)	32.3 (29.9–34.9)	31.5 (29.8–34.5)	0.73
Ascending aorta length, mm	63.8 (57.0–69.1)	63.8 (57.0–69.1)	62.6 (58.1–69.1)	0.91
Sino-tubular junction diameter, mm	28.6 (26.3–31.1)	28.6 (26.3–31.2)	28.3 (26.0–30.7)	0.55
Total aortic valve calcium volume, mm ³	176.1 (42.5–415)	176.1 (40.4–410.7)	204.2 (99.4–453.5)	0.23
Left cusp aortic valve calcium volume, mm ³	61.8 (18.3–167.6)	61.6 (18.2–167.8)	67.1 (26.4–161)	
Right cusp aortic valve calcium volume, mm ³	53.5 (15.3–134.5)	53 (14.9–131.5)	95.6 (26.7–174.5)	0.04
Non-coronary cusp aortic valve calcium, mm ³	86.5 (28.6–203.9)	86 (28–203.6)	118.2 (40.9–249.4)	0.20
LVOT calcium volume, total, mm ³	0.20 (0.0–33.4)	0.20 (0.0–33.9)	0.10 (0.0–26.8)	0.84
Left cusp LVOT calcium volume, mm ³	0.0 (0.0–3.3)	0.0 (0.0–3.2)	0.0 (0.0–5.6)	0.28
Right cusp LVOT calcium volume, mm ³	0.0 (0.0–0.0)	0.0 (0.0–0.0)	0.0 (0.0–0.1)	0.034
Non-coronary cusp LVOT calcium volume, mm ³	0.0 (0.0–0.0)	0.0 (0.0–0.0)	0.0 (0.0–0.3)	0.52
Mitral valve total calcium volume, mm ³	11.9 (0.0–321.9)	11.7 (0.0–308.3)	35.6 (0.0–662.4)	0.17
Mitral anterior leaflet calcium volume, mm ³	0.50 (0.0–56.6)	0.50 (0.0–56.4)	1.80 (0.0–80.3)	0.26
Mitral posterior leaflet calcium volume, mm ³	17.8 (0.0–278.3)	16.9 (0.0–274.3)	34.3 (0.0–649.1)	0.24

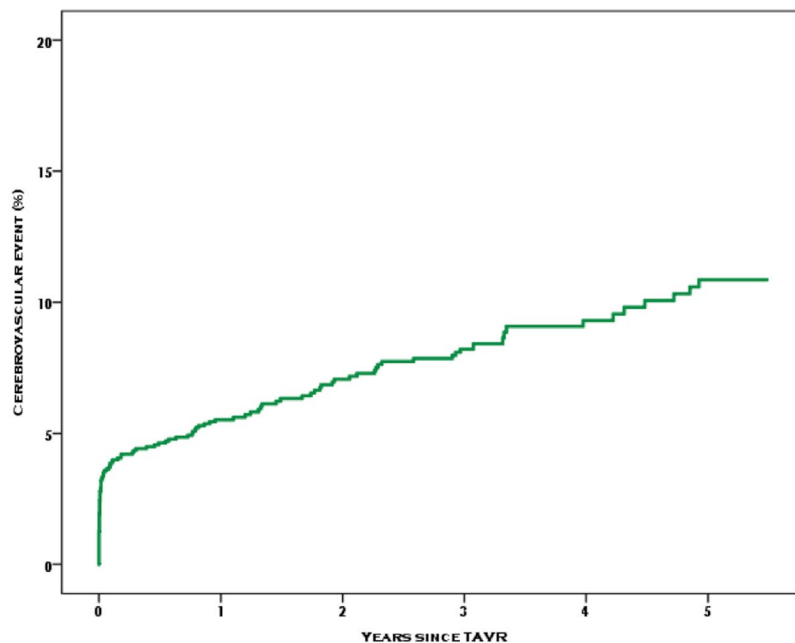
Table 2. Patient CT imaging characteristics. *LVOT* left ventricular outflow tract.

	Day 0	Day 1 to 30 days	> 30 days	Total CVE
CVE, n (%)	19 (1.3)	36 (2.4)	61 (4.1)	105 (7.8)
Disabling stroke, n (%)	15 (1.0)	16 (1.1)	31 (2.1)	62 (4.2)
Non-disabling stroke, n (%)	2 (0.1)	13 (0.9)	15 (1.0)	30 (2.0)
TIA, n (%)	2 (0.1)	7 (0.5)	15 (1.0)	24 (1.6)

Table 3. Incidence of cerebrovascular events. *CVE* cerebrovascular event, *TIA* transient ischemic attack.

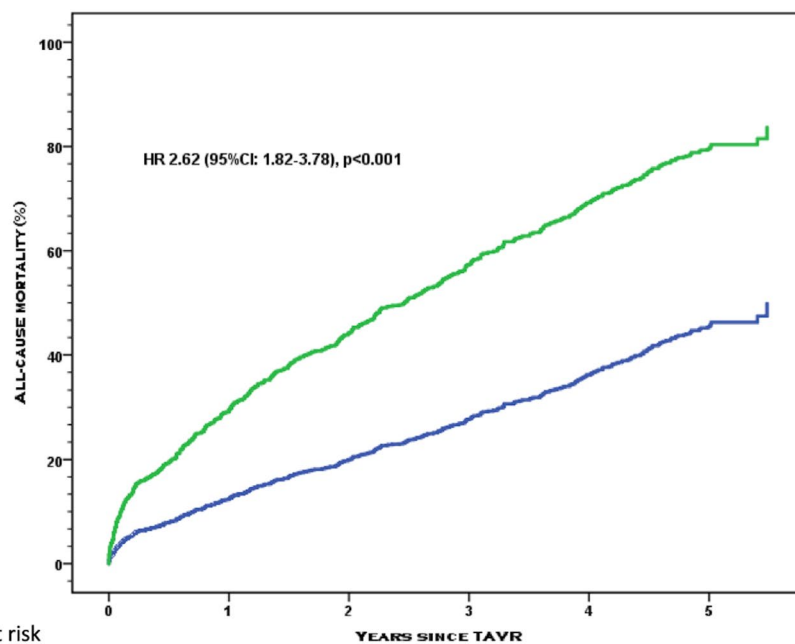
extensive number of patient characteristics. In the present investigation, medical history, symptoms, treatment, imaging and procedural characteristics were entered and analysed using an autoencoder algorithm. Our results suggest an existing ground for the interaction between imaging features such as valve tissue calcification and dimensions of the aortic valve complex, and clinical features to yield CVE. Additional imaging data such as MRI, extensive biological (including per-operative coagulation function estimation or genetics) and environmental profiling may further improve risk assessment. However, the predictive model would require to be adapted for routine clinical practice. The present study is another example of an increasing implementation of machine learning tools to analyse large healthcare databases³².

Limitations. First, the Bern TAVR registry is a manually built database prone to transcription error although our results are consistent with previous reports^{33,34}. Second, frailty indexes are lacking in the present registry and could improve the predictive performance. Third, given constraints relative to our model we could provide only relative variable weighting to explain its functioning⁴. Forth, CT imaging characteristics were obtained using the 3mensio software, however any other software using 3D reconstruction would allow operators to obtain the measurements. Fifth, the cohort studied in the present study is representative of a Western population in a single-center. As the predictors of CVE might differ in a different population because of ethnic, environmental, and genetic factors, that were not recorded in the registry, further external validation in an independent cohort is warranted. Lastly, this is an observational study based on a large prospective TAVR registry including nearly 1500 patients. The occurrence of TAVR-related CVE was however observed in 55 patients only. We used the rare event autoencoder for prediction to address this limitation, however, the small number of events did not allow separate analyses of acute (procedural) and subacute CVE, respectively. Future machine learning research with a larger population is warranted to develop a refined model for predicting TAVR-related CVE.



Number at risk	1,492	1,101	863	639	387	207
----------------	-------	-------	-----	-----	-----	-----

Figure 3. Kaplan–Meier curve of cerebrovascular events after TAVR.



Number at risk						
No CVE	1,437	1,095	957	627	390	201
CVE	55	30	22	14	6	2

Figure 4. Kaplan–Meier curve of all-cause mortality separated by occurrence of cerebrovascular events within 30 days of TAVR.

Conclusions

Despite their complex pathophysiology and rarity, TAVR-related CVE can be predicted by using artificial neural networks. The model is implemented online for broad usage (<https://www.welcome.alviss.ai/#/cvecalculator>). The proposed approach illustrates the potential of artificial intelligence in developing prediction models for multifactorial adverse events such as CVE.

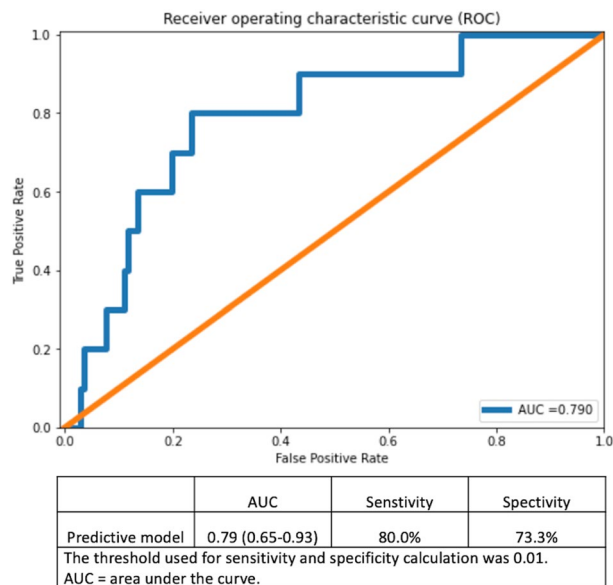


Figure 5. Receiver operating curve of the predictive model. The mean squared error between predicted and known values on the test set was 0.01.

Data availability

The data underlying this article is held at the Clinical Trials Unit of the University of Bern, Switzerland. Data can be made available to external investigators upon request to the corresponding author with permission of the institution, according to local regulations.

Received: 8 April 2021; Accepted: 6 September 2021

Published online: 21 September 2021

References

- LeCun, Y., Bengio, Y. & Hinton, G. Deep learning. *Nature* **521**, 436–444. <https://doi.org/10.1038/nature14539> (2015).
- Hinton, G. Deep learning—a technology with the potential to transform health care. *JAMA* **320**, 1101–1102. <https://doi.org/10.1001/jama.2018.11100> (2018).
- Rajkomar, A., Dean, J. & Kohane, I. Machine learning in medicine. *N. Engl. J. Med.* **380**, 1347–1358. <https://doi.org/10.1056/NEJMr1814259> (2019).
- Quer, G., Arnaout, R., Henne, M. & Arnaout, R. Machine learning and the future of cardiovascular care: JACC state-of-the-art review. *J. Am. Coll. Cardiol.* **77**, 300–313. <https://doi.org/10.1016/j.jacc.2020.11.030> (2021).
- Hannun, A. Y. *et al.* Cardiologist-level arrhythmia detection and classification in ambulatory electrocardiograms using a deep neural network. *Nat. Med.* **25**, 65–69. <https://doi.org/10.1038/s41591-018-0268-3> (2019).
- Hernandez-Suarez, D. F. *et al.* Machine learning prediction models for in-hospital mortality after transcatheter aortic valve replacement. *JACC Cardiovasc. Interv.* **12**, 1328–1338. <https://doi.org/10.1016/j.jcin.2019.06.013> (2019).
- Lopes, R. R. *et al.* Value of machine learning in predicting TAVI outcomes. *Neth. Heart J.* **27**, 443–450. <https://doi.org/10.1007/s12471-019-1285-7> (2019).
- Navarese, E. P. *et al.* Development and validation of a practical model to identify patients at risk of bleeding after TAVR. *JACC Cardiovasc. Interv.* **14**, 1196–1206. <https://doi.org/10.1016/j.jcin.2021.03.024> (2021).
- Nombela-Franco, L. *et al.* Timing, predictive factors, and prognostic value of cerebrovascular events in a large cohort of patients undergoing transcatheter aortic valve implantation. *Circulation* **126**, 3041–3053. <https://doi.org/10.1161/CIRCULATIONAHA.112.110981> (2012).
- Siontis, G. C. M. *et al.* Transcatheter aortic valve implantation vs. surgical aortic valve replacement for treatment of symptomatic severe aortic stenosis: An updated meta-analysis. *Eur. Heart J.* **40**, 3143–3153. <https://doi.org/10.1093/eurheartj/ehz275> (2019).
- Stortecy, S. *et al.* Temporal trends in adoption and outcomes of transcatheter aortic valve implantation: A Swissstavi Registry Analysis. *Eur. Heart J. Qual. Care clin. Outcomes.* **20**, 20. <https://doi.org/10.1093/ehjqcco/qcy048> (2018).
- Van Mieghem, N. M. *et al.* Histopathology of embolic debris captured during transcatheter aortic valve replacement. *Circulation* **127**, 2194–2201. <https://doi.org/10.1161/CIRCULATIONAHA.112.001091> (2013).
- Mohr, J. P. *et al.* American Heart Association Prevention Conference. IV. Prevention and rehabilitation of stroke. Etiology of stroke. *Stroke* **28**, 1501–1506. <https://doi.org/10.1161/01.str.28.7.1501> (1997).
- Liao, Y. B. *et al.* Meta-analysis of the effectiveness and safety of transcatheter aortic valve implantation without balloon predilation. *Am. J. Cardiol.* **117**, 1629–1635. <https://doi.org/10.1016/j.amjcard.2016.02.036> (2016).
- Mentias, A. *et al.* Impact of pre-existing and new-onset atrial fibrillation on outcomes after transcatheter aortic valve replacement. *JACC Cardiovasc. Interv.* **12**, 2119–2129. <https://doi.org/10.1016/j.jcin.2019.06.019> (2019).
- Okuno, T. *et al.* Valvular and nonvalvular atrial fibrillation in patients undergoing transcatheter aortic valve replacement. *JACC Cardiovasc. Interv.* **13**, 2124–2133. <https://doi.org/10.1016/j.jcin.2020.05.049> (2020).
- Miller, D. C. *et al.* Transcatheter (TAVR) versus surgical (AVR) aortic valve replacement: Occurrence, hazard, risk factors, and consequences of neurologic events in the PARTNER trial. *J. Thorac. Cardiovasc. Surg.* **143**, 832–843 e813. <https://doi.org/10.1016/j.jtcvs.2012.01.055> (2012).

18. Fairbairn, T. A. *et al.* Diffusion-weighted MRI determined cerebral embolic infarction following transcatheter aortic valve implantation: Assessment of predictive risk factors and the relationship to subsequent health status. *Heart (British Cardiac Society)* **98**, 18–23. <https://doi.org/10.1136/heartjnl-2011-300065> (2012).
19. Okuno, T. *et al.* Clinical impact of mitral calcium volume in patients undergoing transcatheter aortic valve implantation. *J. Cardiovasc. Comput. Tomogr.* <https://doi.org/10.1016/j.jcct.2020.10.003> (2020).
20. Blanke, P. *et al.* Computed tomography imaging in the context of transcatheter aortic valve implantation (TAVI)/transcatheter aortic valve replacement (TAVR): An expert consensus document of the society of cardiovascular computed tomography. *JACC Cardiovasc. Imaging* **12**, 1–24. <https://doi.org/10.1016/j.jcmg.2018.12.003> (2019).
21. Okuno, T. *et al.* Impact of left ventricular outflow tract calcification on procedural outcomes after transcatheter aortic valve replacement. *JACC Cardiovasc. Interv.* **13**, 1789–1799. <https://doi.org/10.1016/j.jcin.2020.04.015> (2020).
22. Kappetein, A. P. *et al.* Updated standardized endpoint definitions for transcatheter aortic valve implantation: The Valve Academic Research Consortium-2 consensus document (VARC-2). *Eur. J. Cardio-thorac. Surg.* **42**, S45–60. <https://doi.org/10.1093/ejcts/ezs533> (2012).
23. Lansky, A. J. *et al.* Proposed standardized neurological endpoints for cardiovascular clinical trials: An Academic Research Consortium initiative. *J. Am. Coll. Cardiol.* **69**, 679–691. <https://doi.org/10.1016/j.jacc.2016.11.045> (2017).
24. Hain, D. & Jurowetcki, R. Introduction to rare-event predictive modeling for inferential statisticians—a hands-on application in the prediction of breakthrough patents. *arXiv* **2003** (2020).
25. Miok, K., Nguyen-Doan, D., Zaharie, D. & Robnik-Sikonja, M. Generating data using Monte Carlo Dropout. *arXiv* **1909** (2019).
26. Kapadia, S. R. *et al.* Protection against cerebral embolism during transcatheter aortic valve replacement. *J. Am. Coll. Cardiol.* **69**, 367–377. <https://doi.org/10.1016/j.jacc.2016.10.023> (2017).
27. Dangas, G. D. *et al.* A controlled trial of rivaroxaban after transcatheter aortic-valve replacement. *N. Engl. J. Med.* **382**, 120–129. <https://doi.org/10.1056/NEJMoa1911425> (2020).
28. Nijenhuis, V. J. *et al.* Anticoagulation with or without clopidogrel after transcatheter aortic-valve implantation. *N. Engl. J. Med.* **382**, 1696–1707. <https://doi.org/10.1056/NEJMoa1915152> (2020).
29. Brouwer, J. *et al.* Aspirin with or without clopidogrel after transcatheter aortic-valve implantation. *N. Engl. J. Med.* **383**, 1447–1457. <https://doi.org/10.1056/NEJMoa2017815> (2020).
30. Spaziano, M. *et al.* Computed tomography predictors of mortality, stroke and conduction disturbances in women undergoing TAVR: A sub-analysis of the WIN-TAVI registry. *J. Cardiovasc. Comput. Tomogr.* **12**, 338–343. <https://doi.org/10.1016/j.jcct.2018.04.007> (2018).
31. Veulemans, V. *et al.* Novel insights on outcome in horizontal aorta with self-expandable new-generation transcatheter aortic valve replacement devices. *Catheter. Cardiovasc. Interv.* **96**, 1511–1519. <https://doi.org/10.1002/ccd.28961> (2020).
32. Rumsfeld, J. S., Joynt, K. E. & Maddox, T. M. Big data analytics to improve cardiovascular care: Promise and challenges. *Nat. Rev. Cardiol.* **13**, 350–359. <https://doi.org/10.1038/nrcardio.2016.42> (2016).
33. Durand, E. *et al.* Performance analysis of EuroSCORE II compared to the original logistic EuroSCORE and STS scores for predicting 30-day mortality after transcatheter aortic valve replacement. *Am. J. Cardiol.* **111**, 891–897. <https://doi.org/10.1016/j.amjcard.2012.11.056> (2013).
34. Grover, F. L. *et al.* 2016 annual report of the society of thoracic surgeons/American College of Cardiology Transcatheter Valve Therapy Registry. *J. Am. Coll. Cardiol.* **69**, 1215–1230. <https://doi.org/10.1016/j.jacc.2016.11.033> (2017).

Author contributions

P.O., T.P. conceived the study. P.O., T.P. had responsibility for the design of the study. P.O., T.P., T.O., M.A., D.J., S.S., F.P., J.L., G.S., C.G., S.W. were responsible for the acquisition of data. P.O. did the analysis and interpreted the results in collaboration with T.P., S.W. and all other authors. T.O., P.O., T.P. wrote the first draft of the report. All authors critically revised the report for important intellectual content and approved the final version.

Competing interests

Dr. Overtchouk is the CEO of ALVISS.AI SAS. Dr. Windecker serves as unpaid advisory board member and/or unpaid member of the steering/executive group of trials funded by Abbott, Abiomed, Amgen, Astra Zeneca, BMS, Boston Scientific, Biotronik, Cardiovalve, Edwards Lifesciences, MedAlliance, Medtronic, Novartis, Polares, Sinomed, V-Wave and Xeltis, but has not received personal payments by pharmaceutical companies or device manufacturers. He is also member of the steering/executive committee group of several investigated-initiated trials that receive funding by industry without impact on his personal remuneration. Dr. Windecker is an unpaid member of the Pfizer Research Award selection committee in Switzerland. Dr. Pilgrim reports research grants to the institution from Edwards Lifesciences, Boston Scientific and Biotronik, personal fees from Biotronik and Boston Scientific, and other from HighLife SAS. Dr. Okuno reports speaker fees from Abbott. All other authors have no relationships relevant to the contents of this article to disclose.

Additional information

Supplementary Information The online version contains supplementary material available at <https://doi.org/10.1038/s41598-021-98265-5>.

Correspondence and requests for materials should be addressed to P.O.

Reprints and permissions information is available at www.nature.com/reprints.

Publisher's note Springer Nature remains neutral with regard to jurisdictional claims in published maps and institutional affiliations.



Open Access This article is licensed under a Creative Commons Attribution 4.0 International License, which permits use, sharing, adaptation, distribution and reproduction in any medium or format, as long as you give appropriate credit to the original author(s) and the source, provide a link to the Creative Commons licence, and indicate if changes were made. The images or other third party material in this article are included in the article's Creative Commons licence, unless indicated otherwise in a credit line to the material. If material is not included in the article's Creative Commons licence and your intended use is not permitted by statutory regulation or exceeds the permitted use, you will need to obtain permission directly from the copyright holder. To view a copy of this licence, visit <http://creativecommons.org/licenses/by/4.0/>.

© The Author(s) 2021